Available online at www.sciencedirect.com
ScienceDirect
Journal of Contaminant Hydrology 95 (2008) 57–75
JOURNAL OF Contaminant Hydrology
www.elsevier.com/locate/jconhyd

Characterization of subsoil heterogeneity, estimation of grain size distribution and hydraulic conductivity at the Krauthausen test site using Cone Penetration Test

A. Tillmann [a,*], A. Englert [a], Z. Nyari [b], I. Fejes [b], J. Vanderborght [a], H. Vereecken [a]

[a] *Institute of Dynamics and Chemistry of the Geosphere, ICG-IV, Agrosphere, Forschungszentrum Jülich GmbH, 52425 Jülich, Germany*
[b] *Eötvös Lorand Geophysical Institute of Hungary, Department of Engineering Geophysics, P.O. Box 35, H-1440 Budapest, Hungary*

Received 7 June 2006; received in revised form 16 April 2007; accepted 10 July 2007
Available online 17 August 2007

Abstract

A Cone Penetration Test (CPT) survey with a high spatial resolution was performed in order to investigate the stratigraphy as well as the spatial variability of various soil properties of the Krauthausen test site. Analyses of the CPT measurements showed the subsurface to be dominated by a planar layered structure. Variogram analysis of the various CPT parameters disclosed that within each layer the soil properties have an anisotropic spatial correlation structure.

A correlation analysis of the measured CPT data and co-located grain size distributions from soil samples was performed. Since the correlation coefficients were greater equal to 0.7, a reliable empirical relationship between the data sets could be developed. Based on this empirical relationship grain size distributions were estimated at CPT locations. The statistical processing of estimated and measured grain size distributions with respect to their spatial correlation structure disclosed good agreement between the data sets.

The estimated grain size distributions from CPT data were used to estimate the hydraulic conductivity in the aquifer. The results provide detailed information of the spatial heterogeneity of the hydraulic conductivity at Krauthausen test site. The validation of these results, using a prior investigation of hydraulic conductivity statistics, suggests the CPT a fast and inexpensive tool for the estimation of three dimensional hydraulic conductivity fields with sufficient accuracy.

Keywords: Cone Penetration Test; Aquifer characterization; Soil properties; Heterogeneity; Grain size distribution

1. Introduction

To predict flow and transport, the characterization of the physical and chemical heterogeneity of an aquifer is crucial. In particular the hydraulic conductivity's spatial heterogeneity is important, since it is controlling dispersive spreading and mixing of solutes during transport in an aquifer (e.g. Vanderborght and Vereecken, 2002; Russo et al., 2004). However, the estimation of the subsurface spatial heterogeneity is difficult, since local measurements with high spatial resolution are required.

One method to overcome this difficulty in a fast, accurate, and minimally invasive manner is the Cone Penetration Test (CPT), which has become popular in the last decades to investigate shallow unconsolidated sediments (see e.g. Fejes and Jósa, 1990; Lunne et al., 1997). The most valuable characteristic of CPT is its

* Corresponding author. Now at Müller-Boré & Partner, Patent and Trademark Attorneys, Grafinger Str. 2, 81671, Munich, Germany.
E-mail address: a.tillmann@angewandte-geophysik.de (A. Tillmann).

0169-7722/$ - see front matter © 2007 Elsevier B.V. All rights reserved.
doi:10.1016/j.jconhyd.2007.07.013

rapid and accurate way to collect lithological data and quantitative in situ soil properties (e.g. Campanella and Weemees, 1990; Hubbard et al., 2001). A review of available sensors and technologies is given by Bowders and Daniel (1994).

Unfortunately, CPT does not necessarily include local measurements of the hydraulic conductivity. Therefore, we investigated a method to estimate local hydraulic conductivities based on the CPT measurements. The method consists of two steps: First we estimated local grain size distributions based on the CPT measurements, using linear regression. Secondly we linked characteristics of the local grain size distribution to the hydraulic conductivity using empirical formulas provided in the literature.

In particular Hazen (1892), Slichter (1899), Kozeny (1953), Beyer (1964), Bialas and Kleczkowski (1970), Vuković et al. (1992) and others investigated empirical formulas for the determination of hydraulic conductivity of a porous medium from its grain size distribution. From a practical standpoint, this is advantageous, since determination of the grain size distribution is easy and inexpensive and the hydraulic conductivity can be estimated without extensive effort. Although the reliability of these estimates remains an unsolved problem, as discussed in e.g. Sperry and Peirce (1995) and Eggelston and Roistacer (2001), this will not be subject of this work. A discussion of the empirical formulas for various materials most frequently encountered in literature is presented in Vuković et al. (1992).

The present paper is aimed at using CPT data to investigate in detail the spatial heterogeneity of the mechanical resistance, c_r, natural gamma activity, γ, bulk density, ϱ_b, matrix density, ϱ_m, water content, θ, and electrical resistivity, ρ, at the Krauthausen test site, near Jülich, Germany. Moreover it is intended to evaluate the potential of utilizing these CPT measurements for the estimation of local hydraulic conductivities. The paper is organized in the following manner: Section 2 covers the used methodology, i.e. the statistical description of spatial heterogeneity, the relation between grain size distribution and hydraulic conductivity, and the basics of the Cone Penetration Test. Section 3 compiles information on the Krauthausen test site and describes the design of the CPT survey. In Section 4 the results of the CPT survey are shown. The geometry of the layers, the mean values, variances and heterogeneity of each measured parameter within each layer are determined. In Section 5 the geostatistical characteristics of the subsurface's structure is used for kriging, to estimate CPT data at locations where, in a prior survey, soil samples were taken. Thereafter the correlation between kriged CPT data and grain size distributions of the soil samples is analyzed. Proposing a linear relationship, this Section is focused on the estimation of the grain size distribution from in situ measurements with CPT and the evaluation of estimation accuracy. Empirical relations between characteristic grain size distribution parameters and CPT data are given. Some of these relations are presented in detail and subsequently are applied for the estimation of grain size distributions. Using the empirical formula given by Bialas and Kleczkowski (1970) we estimated local hydraulic conductivities based on the 20th percentile of the estimated grain size distributions. The results are compared with heterogeneity estimations of prior investigations. Finally, in Section 6, the results are summarized and conclusions are drawn.

2. Methodology

2.1. Statistical description of spatial heterogeneity

Soil properties do not vary randomly in space, but their variation can be assumed to be gradual and following a pattern that can be quantified using spatial correlation analysis. The variogram is a measure of variability of spatial phenomena and has been used extensively to quantify spatial correlation structures (see e.g. Deutsch, 2002). In the following, the definition of the variogram and related statistics are repeated briefly.

Assuming a set of randomly distributed stationary data values $d_i(\vec{x})$, with known mean m and variance σ^2, the semivariogram is defined as

$$V(d\vec{x}) = \frac{1}{2N}\sum_{i=1}^{N}\left(d_i(\vec{x}) - d_i(\vec{x}+d\vec{x})\right)^2, \qquad (1)$$

where $\vec{x}$ are the coordinates of an observation, $d\vec{x}$ is the distance vector to a second observation, and its length $|d\vec{x}|$ is the lag distance. Eq. (1) describes the dependence of the semivariance from the absolute distance as well as the direction between two observations. Another measure of the spatial variability is the covariance:

$$C(d\vec{x}) = \frac{1}{N}\sum_{i=1}^{N}\left(d_i(\vec{x})\cdot d_i(\vec{x}+d\vec{x})\right) - m^2. \qquad (2)$$

By definition, the covariance at a zero lag distance $C(0)$, is the variance σ^2. With increasing $d\vec{x}$ the covariance typically decreases and finally becomes zero indicating no similarity between points with larger distance. Between the semivariogram and covariance

following relations hold (see e.g. Gringarten and Deutsch (2001)):

$$V(d\vec{x}) = C(0) - C(d\vec{x}) \text{ and} \tag{3}$$

$$C(d\vec{x}) = C(0) - V(d\vec{x}). \tag{4}$$

From these relations it can be concluded, that (a) the sill of the variogram is the variance, which is the variogram value that corresponds to zero correlation; (b) the correlation between $d_i(\vec{x})$ and $d_i(\vec{x}+d\vec{x})$ is positive when the variogram value is less than the sill; and (c) the correlation between $d_i(\vec{x})$ and $d_i(\vec{x}+d\vec{x})$ is negative when the variogram exceeds the sill. For more details on variogram interpretation we refer here to Gringarten and Deutsch (2001).

The results of Eq. (1) are called the experimental variogram. In order to parametrize the average spatial correlation structure, the experimental variogram from measured data values can be fitted with different models (e.g. spherical, exponential, Gaussian, etc.). Deutsch (2002) provides an overview of common variogram models. In the present article the exponential variogram model in combination with the nugget effect variogram model,

$$V(|d\vec{x}|) = C\left(1 - \exp\left(\frac{-|d\vec{x}|}{\lambda}\right)\right) + n, \tag{5}$$

is used, where λ is the correlation length, C is the sill, and n is the nugget.

The meaning of the correlation length λ depends on the variogram model. In contrast, the separation limit of data values, where spatial correlation becomes insignificant, is called the spatial range a (Deutsch, 2002). For asymptotic variogram models, like the exponential model, the spatial range is defined by the distance at which the semivariogram reaches a value of 0.95 times the sill. If the nugget in Eq. (5) is different from zero, the sill plus nugget must be considered for the determination of the spatial range. In this general case the relation between correlation length λ and spatial range a is given by

$$a = -1n\left(0.05\left[1 + \frac{n}{C}\right]\right)\lambda. \tag{6}$$

According to Eq. (6) the spatial range decreases when the nugget effect increases.

2.2. Relation between grain size distribution and hydraulic conductivity

Since sieving analysis of granular sediments is a relatively fast and inexpensive procedure, relationships between the grain size distribution and the hydraulic conductivity are frequently used for estimation of local hydraulic conductivities. Different types of empirical formulas are found in literature. The most common ones are compiled in Table 1.

The most simple formulas, e.g. the one from Hazen (1892) and Bialas and Kleczkowski (1970), only utilize an effective grain diameter d_e, which is taken as d_{10} or d_{20}, i.e. the 10th or 20th percentile of the cumulative grain size distribution. Improved formulas, e.g. in Slichter (1899), also take porosity ϕ into account. More sophisticated formulas make use of a second diameter, e.g. d_{60} in the formula of Beyer (1964), or more parameters of the grain size distribution like in Seiler (1973). The work of Kozeny (1953) or Alyamani and Sen (1993) (not shown in Table 1), for example, steps even beyond these approaches and utilizes the entire grain size distribution curve for the estimation of the hydraulic conductivity. Moreover, Sperry and Peirce (1995) shows that the hydraulic conductivity is, as expected, not only a function of the grain size distribution and the porosity, but also depends on the grain shape. However, Eggelston and Roistacer (2001) compared hydraulic conductivities estimated from grain size distributions with hydraulic conductivities based on air-permeability measurements. They found the mean and the variance of the hydraulic conductivity estimates from grain size distributions at least of the same order of magnitude as those from air-permeability measurements. For both approaches,

Table 1
Selection of empirical relationships to estimate hydraulic conductivity as a function of porosity and grain diameter, with d_{10}, d_{20}, d_{25}, and d_{60} being the 10th, 20th, 25th and 60th quantile of a grain size distribution, and ϕ being the porosity

Source	K	Remarks
Hazen (1892)	$\sim d_{10}^2$	Valid for $0.1 \le d_{10} \le 3$ mm
Slichter (1899)	$\sim \phi^{3.287} d_{10}^2$	Valid for $0.01 \le d_{10} \le 5$ mm
Kozeny (1953)	$\sim \frac{\phi^3}{(1-\phi)^2} d_e^2$	$\frac{1}{d_e} = \frac{3\Delta g_1}{2d_1} + \Sigma_{i=2}^{N} \frac{\Delta g_i}{d_i}$ valid for sands
Beyer (1964)	$\sim \log\left(\frac{500\ d_{10}}{d_{60}}\right) d_{10}^2$	Valid for 0.06 mm $\le d_{10} \le 0.6$ mm
Bialas and Kleczkowski (1970)	$\sim d_{20}^{2.3}$	Valid for $0.2 < \frac{d60}{d10} < 60$
Seiler (1973)	$\sim \left(\frac{d_{60}}{d_{10}}\right) d_{10}^2$	Valid for $\frac{d_{60}}{d_{10}} < 17$
Seiler (1973)	$\sim \left(\frac{d_{60}}{d_{10}}\right) d_{25}^2$	Valid for $\frac{d_{60}}{d_{10}} < 17$

Proportionality factors are omitted.

they found similar spatial correlation of the hydraulic conductivity.

2.3. Cone Penetration Test

Cone Penetration Test (CPT) is a common technique for investigating unconsolidated, near surface sediments. It surveys the subsoil in detail by logging various physical parameters during and after soil penetration. The CPT is used for at least 30 years now and improvement of the technique is ongoing. An overview of the various technical details, equipment and analyses of CPT measurements are given in e.g. Lunne et al. (1997). Here we focus briefly on the specific CPT equipment and procedure used during the CPT survey at the Krauthausen test site:

The self-transport CPT equipment of Elgoscar 2000 Ltd., Hungary, is equipped with a 44 mm string of hollow push rods. At the end of those, a cone penetrometer is fixed. Three electrodes are attached above the cone penetrometer (Fig. 1). During the continuous penetration the cone penetrometer records the mechanical resistance c_r [MPa]. Simultaneously the electrodes are used for electrical resistivity ρ [Ω m] measurements. After the penetration experiment at a certain depth, the string of hollow rods is used to lower a device combining a passive natural gamma probe, a gamma–gamma probe and a neutron probe. This allows for logging the natural gamma activity γ [counts per minute], the gamma–gamma activity and the neutron activity. By calibration, the gamma–gamma activity is then related to the bulk density ϱ_b [kg m^{-3}] and the neutron activity to water content θ (Telford et al., 1990; Fejes and Jósa, 1990; Fejes et al., 1997). Finally the dry matrix density ϱ_m is computed from the bulk density and the water content using the relation $\varrho_m = \varrho_b - \varrho_f \cdot \theta$, where ϱ_f is the fluid density. Furthermore Fejes et al. (1997) uses the natural gamma activity to classify the soil into gravel/sand, silt and clay, where gamma activities ≤ 800 counts/min (sand limit) indicate sand and gravel and activities ≥ 1700 counts/min indicate clay. Silt typically has intermediate values.

Fig. 1. Cone Penetration Test (CPT) equipment (Elgoscar 2000 Ltd.) used at Krauthausen test site: 1. cone penetrometer, 2. three electrodes, 3. hollow push rods.

3. Field campaign

3.1. Test site Krauthausen

The Krauthausen test site is situated approximately 10 km northwest of the city of Düren and 8 km from Jülich, Germany. It has an extension of 200 m × 70 m and is covered with grass. The field site is located in the southern part of the Lower Rhine Embayment, where Quaternary sediments are mostly fluvial deposits from the river system of Rhine and Maas covered by aeolian sediments. The fluvial sediments are characterized by a sequence of permeable and impermeable layers representing a typical multi-layer aquifer system. Due to northwest–southeast striking faults, the Lower Rhine Embayment is divided into several tectonic compartments. The Krauthausen test site is located on a small inserted block between the Rur block and the Erft block.

The test site was set up in 1993 by the Forschungszentrum Jülich (as described in detail by Döring, 1997; Vereecken et al., 1999, 2000; Englert, 2003) to experimentally study water flow and solute transport processes. Studies at Krauthausen test site focused on the uppermost aquifer in a depth from 2 m to 11 m. The aquifer material consists mainly of gravelly and sandy sediments deposited by a local braided river system of the river Rur, which are on top of the Rhine and Maas sediments. The clay and silt content of the aquifer sediments vary between 0.5% and 7.5%, the mean total porosity is 26 ± 7%, and the overall mean hydraulic conductivity is about $3.8 \cdot 10^{-3}$ m/s. (Vereecken et al., 2000). The local base of the aquifer in a depth of 11 m to 13 m consists of intermittent thin layers of clay and silt.

For monitoring and sampling purposes 75 boreholes of 324 mm diameter were deepened using dry rotary drilling,

and observation wells of 50 mm diameter were installed (for details see Vereecken et al., 1999). Seven drillings were sampled completely (10 and 20 cm sampling intervals), three of them (number B07, B22, and B32) are located within the CPT survey area (Fig. 2). The other drillings were sampled only at several depths or were not sampled at all. The horizontal sampling interval of the Krauthausen observation well set up was approximately 5 m. Vereecken et al. (2000) analyzed the grain size distributions of those soil samples and applied the formula of Seiler (1973) to estimate hydraulic conductivities. Results of Vereecken et al. (2000) were used as a prior information for the CPT survey design, and will be later on used for the validation of the results of the present

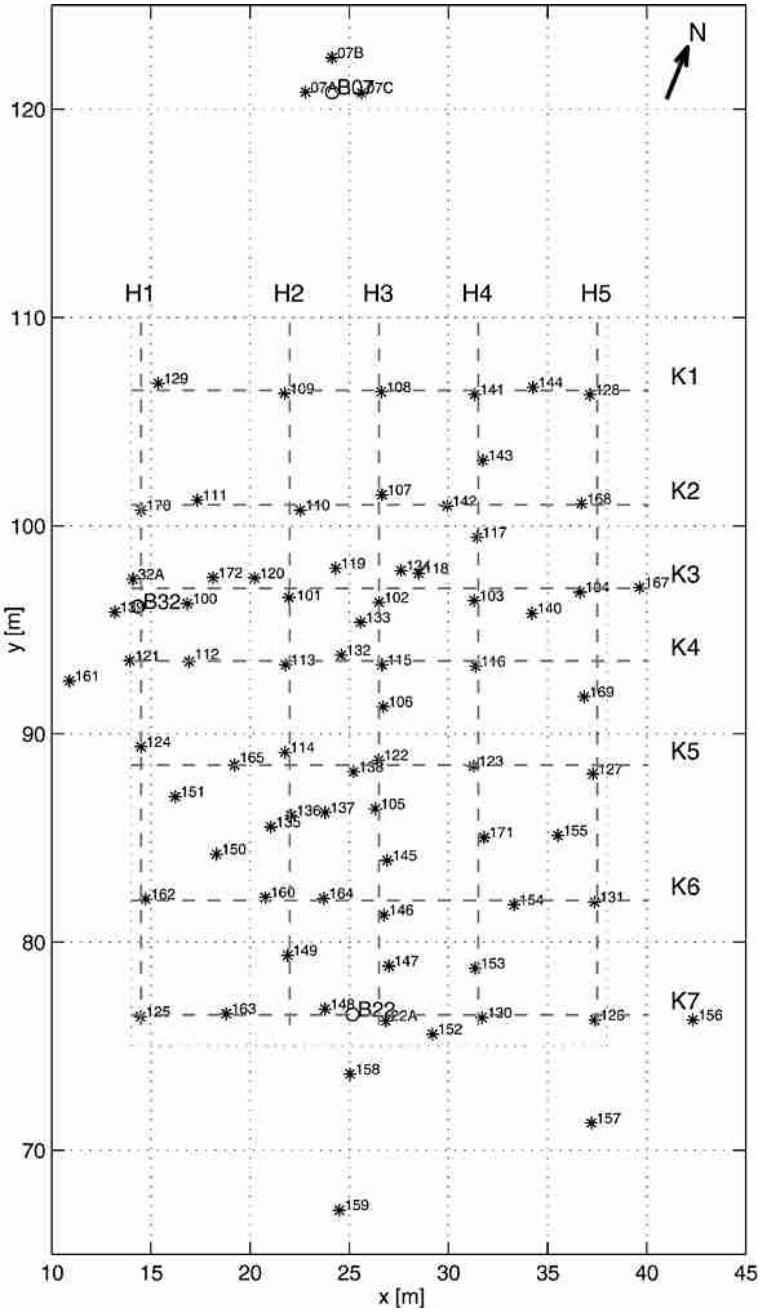

Fig. 2. Layout of the CPT survey at Krauthausen test site: Locations of the boreholes B07, B22, and B32 are marked as circles. The Cone Penetration Test locations are marked by asterisks and numbered in chronological order. Cross section H3 is shown in detail in Figs. 3 and 4.

study (see Section 5.3). As indicated in Section 2.2, the estimation of hydraulic conductivity from grain size distributions can be difficult. However, for the Krauthausen sediments Englert (2003) showed a fairly good agreement between the geometric mean of the hydraulic conductivities from the Vereecken et al. (2000) grain size distributions, i.e. $K = 1.4 \cdot 10^{-3}$ m/s, and the hydraulic conductivity inferred from a pumping test, i.e.: $K = 3.8 \cdot 10^{-3}$ m/s.

3.2. The CPT survey

In a central area of 30 m × 20 m of the test site Krauthausen, shown in Fig. 2, 78 Cone Penetration Tests were performed down to 13.5 m depth average and 16 m depth maximum (see also Tillmann et al., 2004). The horizontal sampling interval was in the range from 1.5 m to 3 m to achieve a good estimation of the small scale variability. The vertical sampling interval was 10 cm. The push velocity

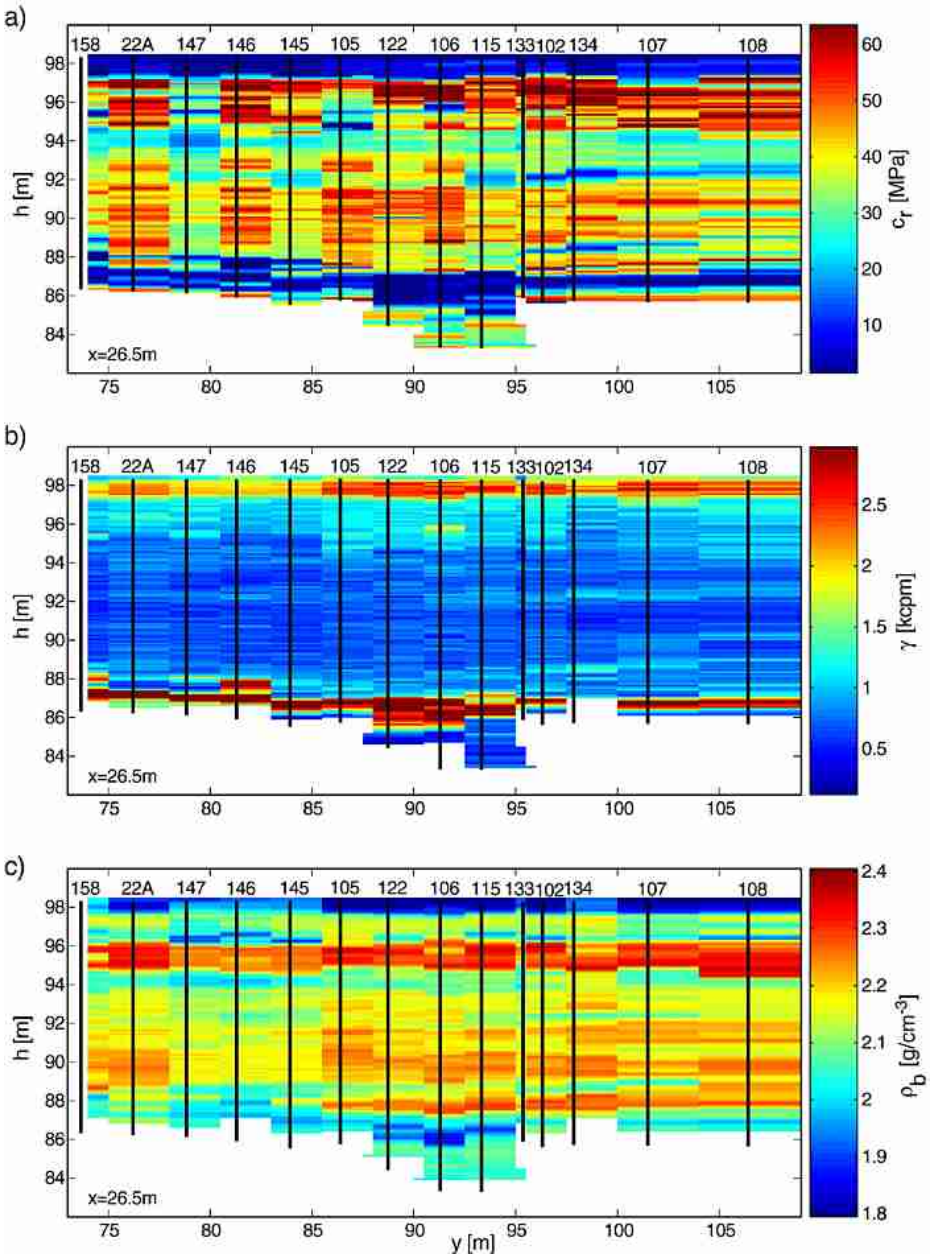

Fig. 3. Cross section H3 of the CPT survey at Krauthausen test site with height, h, given in meters above mean sea level (MSL). Top: mechanic cone resistance, c_r, middle: natural gamma activity, γ, bottom: bulk density, ϱ_b.

was about 1 cm/s. During the push procedure the mechanic cone resistance c_r [MPa] and the electrical resistivity ρ [Ω m] are measured. After pushing the natural gamma, the gamma–gamma and the neutron activity was logged inside the pipe also with a vertical spacing of 10 cm. Post processing of the gamma–gamma and the neutron activity to convert the radiation data into bulk density and water content was performed by Elgoscar 2000 Ltd. in Budapest, Hungary (Fejes et al., 1997).

4. Heterogeneity of direct measured sediment properties

4.1. Layering of the Krauthausen subsurface

To analyze the CPT measurements in a qualitative way, cone resistance, c_r, natural gamma activity, γ, bulk density, ϱ_b, water pore content, θ, and, where available, the electrical resistivity, ρ, logs were gathered into cross

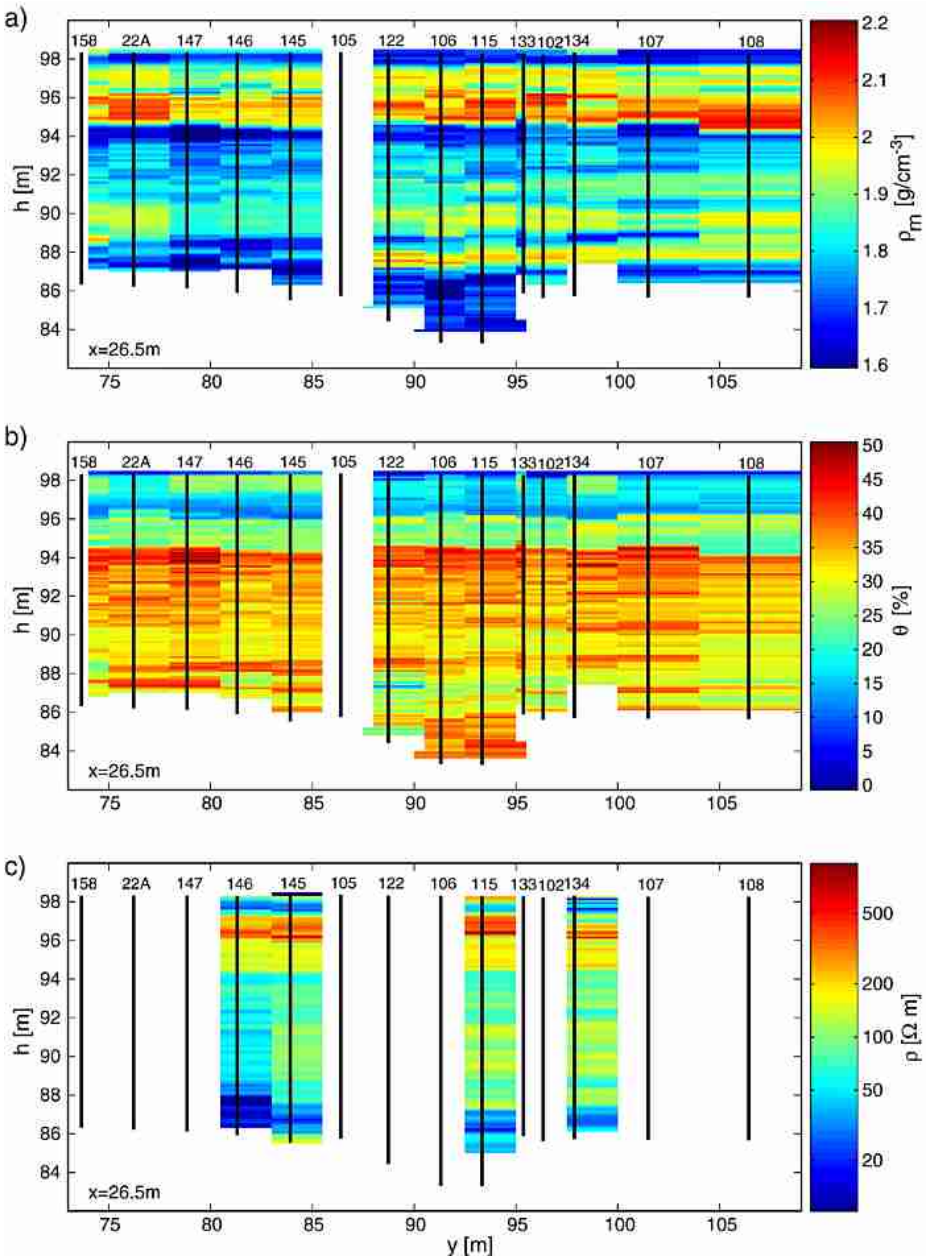

Fig. 4. Cross section H3 of the CPT survey at Krauthausen test site with height, h, given in meters above mean sea level (MSL). Top: dry matrix density, ϱ_m, middle: water content, θ, bottom: electrical resistivity, ρ.

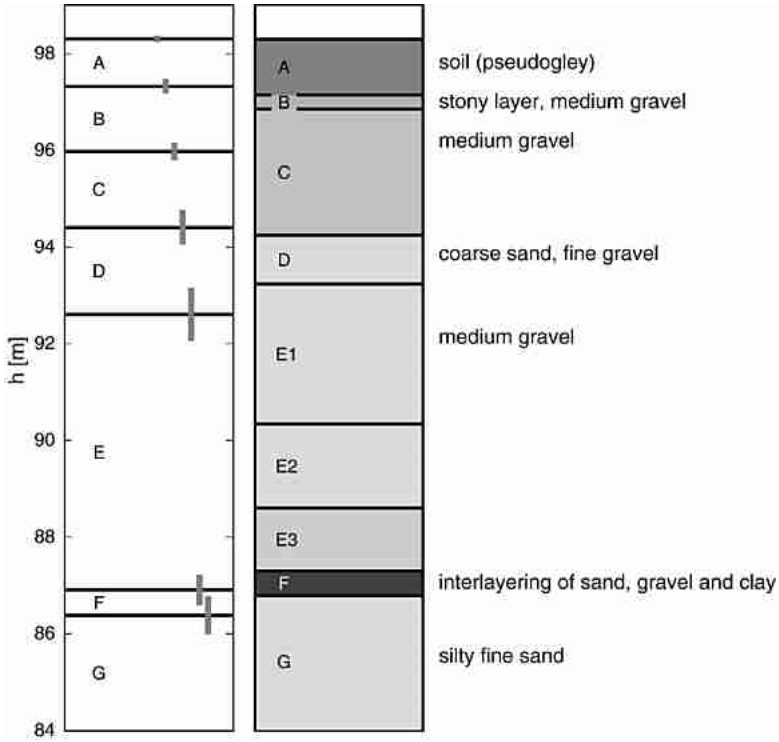

Fig. 5. Layering of the Krauthausen test site according to the CPT survey (left) and after Döring (1997) (right) with height *h* given in meters above mean sea level (MSL).

sections. The cross section H3 has the highest spatial sampling density and is shown in Figs. 3 and 4 exemplarily. A more detailed description of the data including plots of all cross sections is provided by Tillmann (2005). Figs. 3 and 4 show the soil parameters in a nearest neighbor interpolation together with the associated CPT locations. The most striking layer boundary in the figures is at about 94.3 m elevation above mean sea level (MSL). For this boundary, as for the other boundaries, a variability in elevation above mean sea level of less than 0.5 m is detectable. Based upon the cross sections H1–H5 and K1–K7 in Fig. 2, a geological interpretation in terms of a manual separation into homogeneous layers was performed for every CPT location. Fig. 5 shows the stratified geological model of seven layers, which are marked from top to bottom with letters from A to G. In Fig. 5 error bars indicate the variability of boundaries, based on the standard deviation of the layer boundaries elevation of all individual CPT locations. The mean thickness of each layer, its top elevation above MSL and the standard deviation of both are displayed in Table 2. Here the geological structure of the test site is treated as a perfectly stratified model.

A generalized continuous model is formed by averaging the measured values of all CPT logs based on depth intervals of 10 cm. The generalized CPT logs of the various physical properties and their overall statistical distribution are shown in Fig. 6. The results from the CPT survey shown in Figs. 5 and 6 and Tables 2 and 3 were related to the generalized stratification as found by Döring (1997) from field lithological logs, observed during the drilling of the well bore. In this context the stratified model can be characterized in short:

The top soil layer, layer A, is characterized by a high value of natural gamma activity, a low cone resistance of about 5 MPa, and a low electrical resistivity of approx.

Table 2
Generalized stratification (layer A–G) of the subsurface at Krauthausen test site, including *d*, the mean layer thickness, and *h*, the layers top elevation above MSL

	d [m]	*h* [m]	Material
A	0.98±0.16	98.31±0.07	Soil (pseudogley)
B	1.35±0.19	97.33±0.15	Stony layer, medium gravel
C	1.58±0.37	95.98±0.18	Medium gravel
D	1.86±0.54	94.41±0.36	Coarse sand, fine gravel
E	5.68±0.62	92.61±0.55	Medium gravel
F	0.52±0.18	86.91±0.32	Inter-layering of sand, gravel and clay
G	–	86.38±0.39	Silty fine sand

The layer material listed is according to Döring (1997).

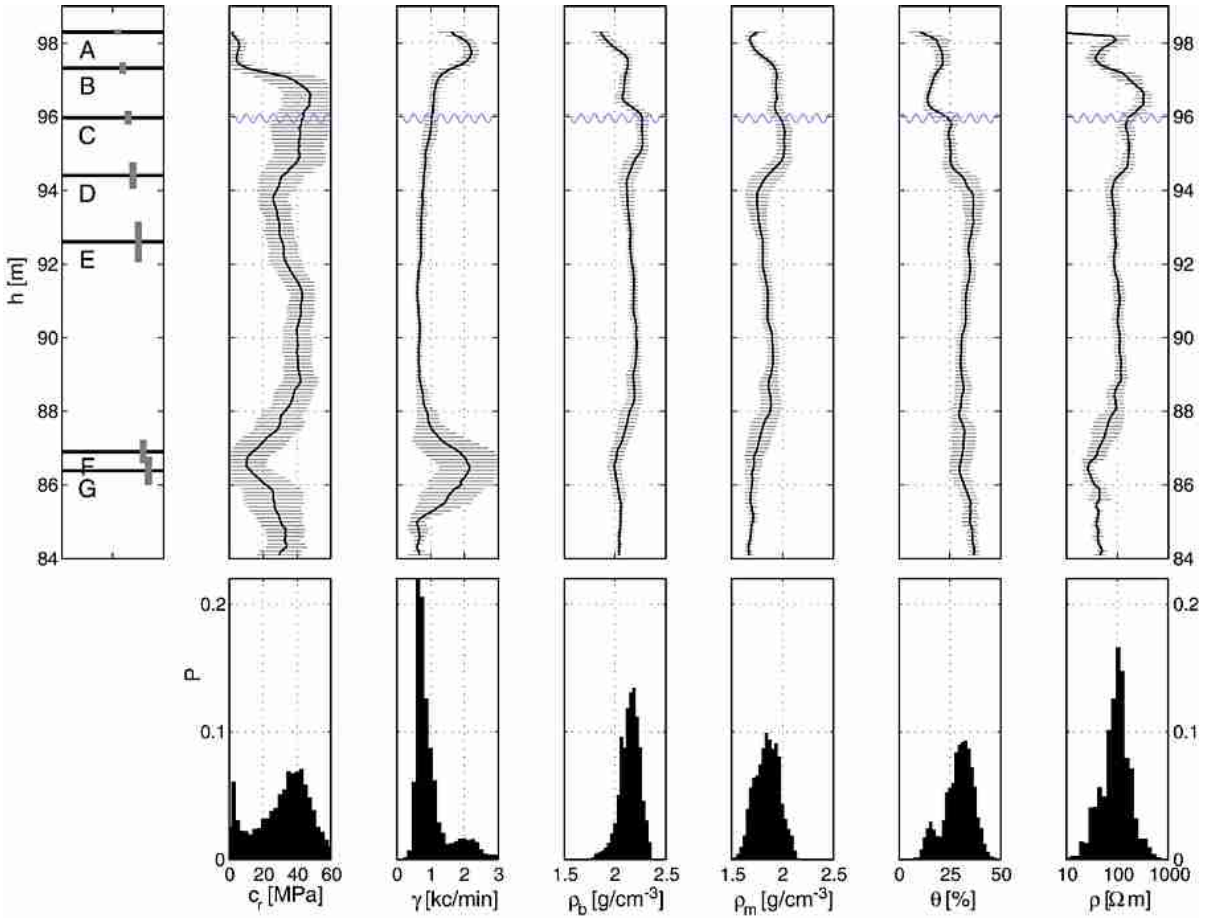

Fig. 6. One dimensional generalized model from interval-wise averaged CPT logs at Krauthausen test site, including the mechanical resistance, c_r, natural gamma activity, γ, bulk density, ϱ_b, matrix density, ϱ_m, water content, θ, and electrical resistivity, ρ. The solid line displays the mean value of each CPT datum and the shaded bars its standard deviation. h indicates the height above mean sea level (MSL). The histogram of each parameter is displayed below the accordant CPT-log. The undulating lines in the logs indicate the water table. For comparison, the layering (layer A–G) is included in the figure.

50 Ω m, which indicates a significant clay content within the soil.

Layer B is separated from layer A by a well defined sharp inter-layer boundary. The material of layer B can be identified as gravel or debris because of a very high mean cone resistance (≈46 MPa), the high electrical resistivity (≈300 Ω m) and a typical bulk density of about 2.1 g/cm^3. Since its natural gamma activity level is higher than the so called sand limit of 800 cpm (see Section 2.3), the layer material must contain either a

Table 3
Mean values and standard deviations of soil properties within the layers A to G at Krauthausen test site, including the mechanical resistance, c_r, natural gamma activity, γ, bulk density, ϱ_b, matrix density, ϱ_m, water content, θ, and electrical resistivity, ρ

	c_r [MPa]	γ [counts]	ϱ_b [t/m^3]	ϱ_m [t/m^3]	θ [%]	$\log_{10}$ (ρ/Ω m)
A	5.0±4.0	2106±253	1.96±0.11	1.76±0.09	20.2±4.8	1.73±0.26
B	46.3±15.8	1095±155	2.10±0.08	1.94±0.06	16.2±4.6	2.44±0.19
C	40.1±15.4	894±187	2.24±0.08	1.99±0.11	25.8±4.2	2.19±0.14
D	29.6±8.3	717±133	2.14±0.05	1.78±0.07	35.8±3.8	1.95±0.08
E	37.4±11.6	746±309	2.18±0.07	1.86±0.09	31.9±3.8	1.98±0.17
F	11.2±12.2	2041±1004	2.03±0.07	1.72±0.09	30.7±5.5	1.52±0.19
G	28.5±14.8	1172±784	2.04±0.05	1.69±0.05	35.0±3.7	1.63±0.12

certain amount of clay minerals or the gravel material itself has a higher gamma activity than average.

Layer C consists more or less of the same material as layer B and the changes of the material properties can be explained as effect of the water table, which is observed at the depth of the layer B–C boundary. The mechanical cone resistance is decreasing and the dry matrix density is increasing across the B/C boundary for about 5 to 10%, which may indicate a slight change in material. Döring (1997) proposed a medium gravel layer across the layer B/C boundary topped by a stony layer. This stony layer was not found in the CPT data rather stones were found in the entire layer B and C causing a very high variance in the cone resistance data. Due to the higher water content in layer C the bulk density increases in combination with a decrease of electrical resistivity by factor 2.

Unlike the above layers, layer D is characterized by a low natural gamma activity (below the sand limit of 800 cpm), a lower cone resistance of about 30 MPa, and a high water content. Therefore layer D seems to consist of a well sorted sand.

Layer E, 4.3 m to 6.4 m thick, is the thickest layer of the investigated volume. A further stratification like proposed by Döring (1997) was not confirmed by the CPT survey. The layer's natural gamma activity is below the sand limit of 800 cpm. The average cone pressure (38 MPa) and resistivity (200 Ω m) values are typical for a sandy gravel or a gravely sand. Since both parameters show a high variance within layer E, it is assumed that layer E is built up from a thin layered stratification with varying sand to gravel ratio.

Layer F is a less permeable layer, i.e. base of the upper aquifer. The high average natural gamma activity (2200 cpm, which is significantly higher than the clay limit of 1700 cpm) and the very low cone resistance (5 MPa, with a high variability) is typical for clay. Since its resistivity value is higher than usual, it can be assumed that the layer may have other components besides clay, i.e. more or less distinct local sandy inclusions.

The investigated area below the layer F is treated as indefinite, since the bottom of layer G was not reached. According to the measured intermediate cone resistance and gamma activity it seems to be sandy gravel or gravely sand.

4.2. Heterogeneity within the layers

Dominated by the planar structure, the CPT measurements showed the subsoil variable in each layer (Table 3 and Fig. 6). The characterization of the spatial variability, i.e. the spatial correlation structure, was performed on the soil properties measured during the CPT survey using variogram analysis (Section 2.1). Since the sampling density differs an order of magnitude for the horizontal and vertical directions, the analysis was performed for both directions independently. To enforce statistical stationarity of the data, the mean value and a linear trend were removed from the data prior to variogram analysis, and the residuals were transformed to a Gaussian distribution with unit variance using a normal score transform (see e.g. Goovaerts and Jacquez, 2004). Additionally, data values outside of the 95% confidence interval were treated as outliers and were eliminated from the data set prior to the normal score transform.

The variograms in the horizontal direction were calculated for 17 layers of 0.5 m thickness in between 88 m and 96 m above MSL. To resolve potential anisotropy in the horizontal spatial correlation structure, the distance vectors were sorted after length and direction, i.e. azimuth angle in cylindrical coordinates. The distance vectors were gathered into overlapping segments of ±30° angle and including a ±0.5 lag tolerance. The increment between each segment is 10° and 0.5 m. For each measured parameter, 306 variograms were obtained and fitted with the combined exponential-nugget model, Eq. (5). From those fits, the respective sills, nuggets and the lateral correlation lengths were derived and presented in Fig. 7.

The sill value for all variograms in horizontal direction was 1 including variations of only 0.04, which was to be expected, since the data were normal score transformed. Therefore no further investigation on the sill distribution was performed. The nugget was in general below 0.1 except for c_r and ϱ_m at elevations of about 94.5 m above MLS and azimuth angles regarding to the north–south direction. For these positions nugget values of 0.5 and larger occurred, indicating a small scale variability of the cone resistance and bulk density in the transition zone of layers C and D.

The spatial range a was computed from the correlation length and nugget using Eq. (6). The mean range a in horizontal direction and its standard deviation as a function of depth is displayed in Fig. 7a, d and g. Its depth–azimuth distribution is shown in Fig. 7b, e and h. The depth–azimuth distribution of the nugget is shown in Fig. 7c, f and i. The mean spatial range function $a(z)$ has a similar shape for all material properties. Typically the spatial range varies between 2 m and 7 m for all material properties. An exception is the bulk density data in layer D (92.6 m to 94.4 m above MLS), showing higher spatial ranges of about 10 to 20 m in combination with a dominating nugget effect (see Fig. 7i).

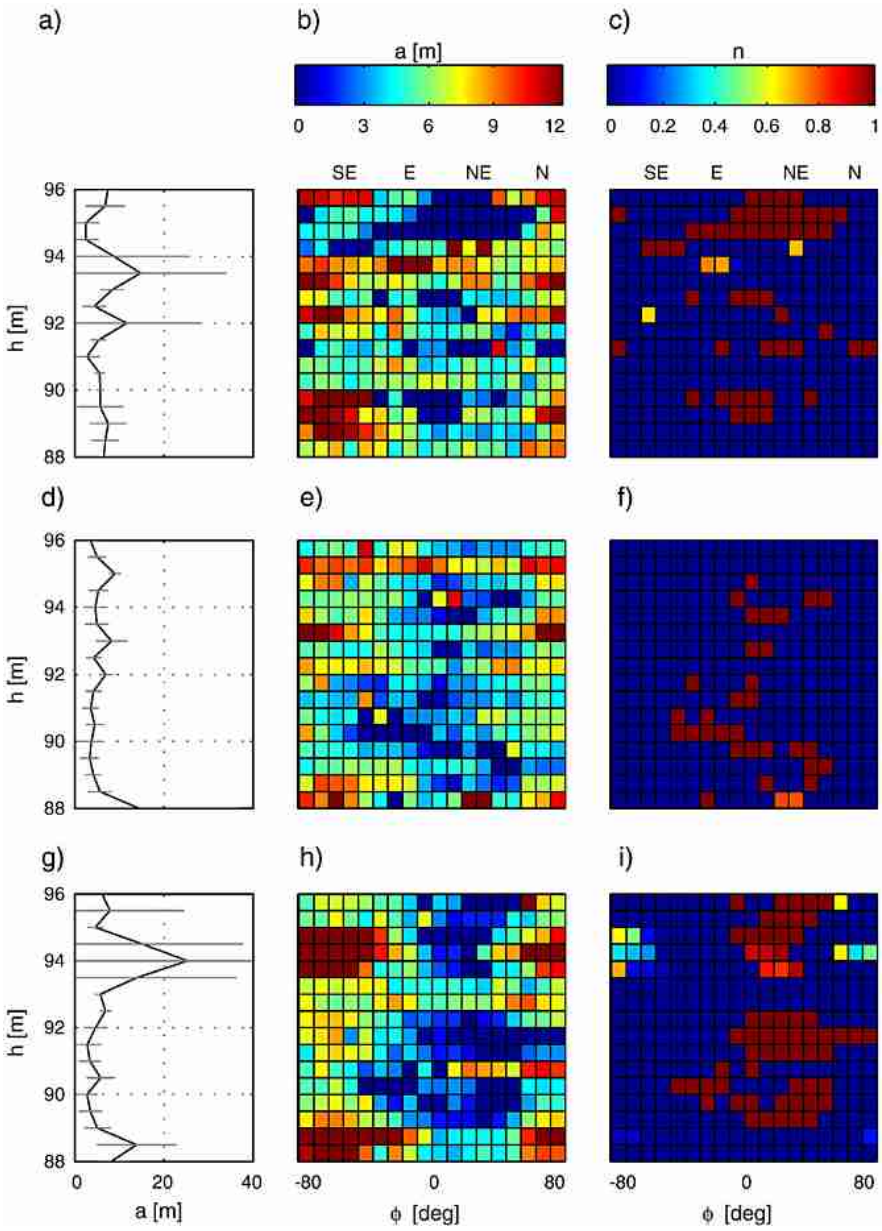

Fig. 7. Characteristic parameters from anisotropic variogram fitting in horizontal direction of CPT measurements at Krauthausen test site, including the mechanical resistance, c_r, natural gamma activity, γ, and the dry grain matrix density, ϱ_m. a,d,g) show the mean range and it's standard deviation versus depth, b,e,h) show the range versus azimuth and depth, and c,f,i) show the nugget versus azimuth and depth for the material properties c_r, γ, and ϱ_m, respectively.

Examining a as function of azimuth, as shown in Fig. 7b, e and h, a complex structure can be observed. The most distinct anisotropic behavior can be observed for the natural gamma activity γ and the dry grain matrix density ϱ_m. For all elevation levels and for azimuthal ranges of $-20°$ to 50°, that is the east to northeast direction, a spatial range lower than 4 m can be observed. In some cases the spatial range tends to zero along with a nugget close to 1. In contrast, the spatial range in southeast to south direction is typical about 5 to 9 m, at elevation levels below 89 m and from 93.5 to 95 m even larger with peak values up to 30 m. The mechanical cone resistance data c_r show similar statistical anisotropic behavior, but not as uniform as γ and ϱ_m.

The variograms in vertical direction were calculated within geologically homogeneous layers C, D, and E

according to Table 2. The other layers were not considered since they either do not belong to the aquifer or are too thin for a reliable variogram analysis. With respect to the high spatial sampling of data, the lag tolerances were chosen to 0.15 m and the lag distance increment to 0.10 m. The results of the fitting using the exponential-nugget correlation structure model according to Eq. (5) are compiled in Table 4. Except the sill value, the geostatistical parameters in Table 4 vary more between the CPT measured properties than between layers. This indicates comparable spatial correlation length (λ) and range (a) in vertical direction, that is $\lambda = 0.42 \pm 0.06$ m, and $a = 1.2 \pm 0.17$ m in layer C, $\lambda = 0.39 \pm 0.17$ m and $a = 1.1 \pm 0.5$ m in layer D, and $\lambda = 0.41 \pm 0.25$ m and $a = 1.2 \pm 0.7$ m in layer E. Including variability in between the CPT measured properties, the sill value is fluctuating around 1, like in the horizontal variograms for layer C only. Layer D and E show the CPT measured properties fluctuating around sill values <1, indicating a zonal anisotropy. Except the spatial correlation model for θ and ρ in Layer C, the nuggets are small ($n \leq 0.17$), indicating only small variability not resolved with the CPT measurements in vertical direction.

It can be summarized that the spatial correlation structure's statistical anisotropy is not limited to differences between spatial correlation in vertical and horizontal direction, but includes anisotropy of the spatial correlation in horizontal directions as function of depth and azimuth. This is likely for fluvial deposits like the sediments of test site Krauthausen, which is part of the braided river system of the river Rur. Although a detailed knowledge on the sedimentary structures of the system of the river Rur is not available, the studied anisotropy of the correlation lengths at Krauthausen test site is in accordance with the expected orientation of sedimentary bodies. Namely the longest correlation length in mean flow direction of the river Rur, shorter correlation length perpendicular to the mean flow direction and the shortest correlation length in vertical direction.

Table 4
Fitting parameters of the variograms in vertical direction, computed for CPT logs at Krauthausen test site in layers C, D, and E. The CPT measurements include the mechanical resistance, c_r, natural gamma activity, γ, bulk density, ϱ_b, matrix density, ϱ_m, water content, θ, and electrical resistivity, ρ

	c_r	γ	ϱ_b	ϱ_m	θ	ρ
Layer C						
C	0.87	0.68	1.14	1.33	0.97	0.90
n	0.15	0.17	0.00	0.01	0.23	0.31
λ	0.46	0.36	0.37	0.50	0.41	0.47
a	1.31	1.00	1.11	1.48	1.13	1.27
Layer D						
C	0.85	0.83	0.98	0.93	0.64	0.89
n	0.13	0.12	0.04	0.04	0.05	0.12
λ	0.67	0.26	0.44	0.49	0.19	0.32
a	1.92	0.73	1.29	1.45	0.55	0.91
Layer E						
C	0.72	0.77	0.72	0.76	0.77	0.15
n	0.07	0.07	0.13	0.04	0.03	0.01
λ	0.29	0.19	0.56	0.38	0.20	0.85
a	0.84	0.55	1.58	1.12	0.59	2.50

The fitting parameters are the sill, C, the nugget, n, the spatial correlation length, λ, and the spatial range, a.

5. Estimation of the grain size distribution

5.1. Deducing grain size distribution from CPT measurements

To examine the correlation between grain size distributions from sieving analyses of core samples and CPT data, co-located data are needed. Therefore, CPT measurements were investigated in the vicinity of the boreholes B07, B22, and B32 (see Fig. 2). These boreholes were sampled during drilling. Within a circle of approximately 5 m diameter around the boreholes B07, B22, and B32, minimum three CPT measurements were performed. For technical reasons a minimum distance of 1.5 m have to be kept to prevent damage of the existing borehole casing. Since the CPT data and the drilled boreholes are not exactly co-located, CPT parameter were estimated for locations where soil samples were taken from using kriging. For that purpose the variogram analyses of Section 4.2 were utilized. Since the variogram analyses showed a distinct anisotropy in the spatial correlation structure, the ordinary kriging method (see e.g. Isaaks and Srivastava, 1989; Stein, 1999; Chilès and Delfiner, 1999) was applied to the data set to obtain estimated CPT logs at the borehole locations. Fig. 8a–e show the estimated CPT measurements at the locations B07, B22, and B32, where the about 250 soil samples were taken independently. Fig. 8f shows the according cumulative grain size distribution obtained from sieving of the soil samples.

In order to quantify the relationship between CPT and core sample data a correlation analysis of the values of the estimated CPT logs, except for the electrical resistivity, and various grain size parameters were performed. The correlation analyses were based on all available data, i.e. the 250 soil samples and the co-located estimates from CPT measurements. The grain size probability density distribution (PDF) $\log_{10}p(d_g)$, the cumulative density distribution (CDF) $\log_{10}(d_g)$,

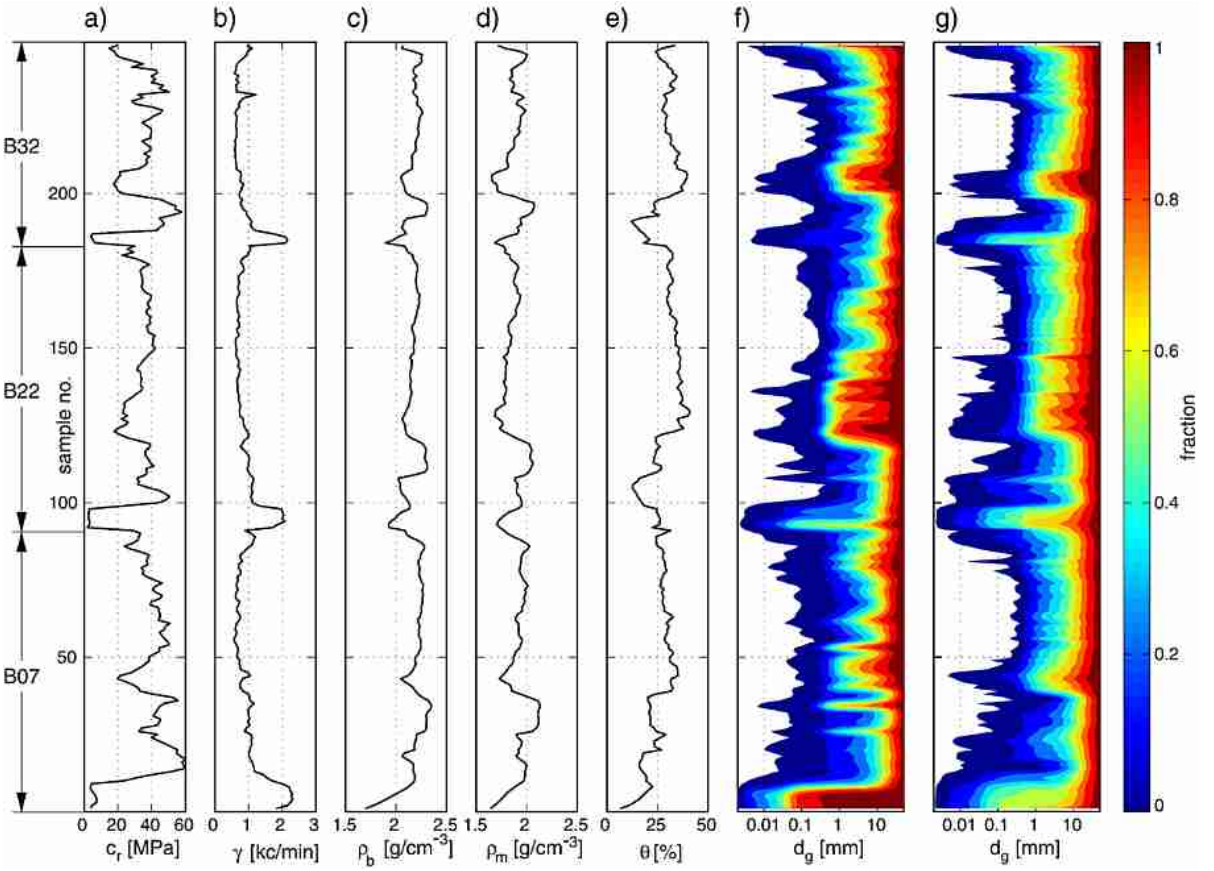

Fig. 8. Co-located CPT measurements, grain size distributions from sieving analysis and estimated grain size distributions based on CPT measurements at Krauthausen test site: a)–e) estimated CPT logs for the core sample locations, including mechanical resistance, c_r, natural gamma activity, γ, bulk density, ϱ_b, matrix density, ϱ_m, and water content, θ. f) cumulative grain size distribution (CDF) derived from core samples, and g) estimated CDF from CPT measurements using multiple regression.

and the percentiles $\log_{10}d_{\%}$ of the CDF were used for correlation. The common logarithm of the grain size distributions and the percentile diameter is used since their values follow a log-normal distribution. For the analysis a linear relationship between $c_r(\vec{x})$, $\gamma(\vec{x})$, $\varrho_b(\vec{x})$, $\theta(\vec{x})$, and $\varrho_m(\vec{x})$, and the core sample data $\log_{10}p(\vec{x},d_g)$, $\log_{10}P(\vec{x},d_g)$, and $\log_{10}d_{\%}$ is assumed.

In a first step the bi-variate correlation between CPT measurements and relevant mass fractions of the sample's grain size distributions, expressed in probability density distributions (PDF) and cumulative grain size distributions (CDF) were analyzed (Tables 5, 6 and 7). Comparing the correlation coefficients of each CPT measurement method, in descending order, the natural gamma activity γ, mechanical cone resistance c_r, and bulk density ϱ_b turned out to be the parameters with the highest correlation to the grain size distribution. Comparing the results in Tables 5 and 6 it can be noticed, that the correlation to the CDF produces higher correlation coefficients for grain sizes up to 0.5 mm. For grain diameters between 0.5 mm and 2 mm the PDF showed a better correlation to the CPT data than the CDF. The correlation coefficients for the percentiles of the CDF in Table 7 show a good correlation up to the 20th percentile. This percentile is associated with a mean grain diameter of 0.36 mm conforming to the grain diameter range of high correlation with the CDF. However, even for CDF data the correlation decreases rapidly, especially for the natural gamma activity, for grain diameters d_g larger than 0.2 mm. Since the bi-variate correlation between CPT measurements and grain sizes of coarse sand and gravel are obviously smaller then correlations with sand, silt and clay fractions, the estimation of grain sizes of coarse sand and gravel are expected to be less certain.

In a second step multiple regression was used for an enhanced estimation of grain size distributions based on the CPT measurements. Thereto the natural gamma

Table 5
Results of correlation analyses at Krauthausen test site: Bi-variate correlation coefficients between the grain size probability distribution (PDF) from sieving and CPT data, including mechanical resistance, c_r, natural gamma activity, γ, bulk density, ϱ_b, matrix density, ϱ_m, and water content, θ

d_g [mm]	0.002	0.01	0.02	0.05	0.1	0.2	0.5	1	2	5	20
c_r	−0.66	−0.27	−0.38	−0.51	−0.41	−0.11	0.11	0.32	0.49	0.36	0.38
γ	0.72	0.59	0.65	0.67	0.51	−0.04	−0.51	−0.79	−0.83	−0.31	−0.18
ρ_b	−0.60	−0.24	−0.32	−0.43	−0.24	0.07	0.18	0.30	0.45	0.43	0.38
θ	−0.23	−0.53	−0.53	−0.36	−0.25	0.19	0.56	0.64	0.47	0.02	−0.14
ρ_m	−0.39	0.11	0.05	−0.15	−0.05	−0.05	−0.18	−0.14	0.10	0.36	0.43
$\chi_{(p(d_g)^*,\ p(d_g))}$	0.79	0.63	0.69	0.68	0.54	0.26	0.60	0.83	0.84	0.46	0.46
$\sigma_{(p(d_g)^*-p(d_g))}$	0.16	0.51	0.42	0.42	0.27	0.27	0.28	0.25	0.26	0.38	0.53

Parameter $\chi_{(p(d_g)^*,\ p(d_g))}$ denotes the multivariate correlation coefficient between grain size probability distribution from sieving and it's estimation based on CPT data. Parameter $\sigma_{(p(d_g)^*-p(d_g))}$ denotes the standard deviation of the difference between the multivariate estimate and the 'true' grain size distribution, i.e. the standard deviation of the error.

activity γ, mechanical cone resistance c_r, and bulk density ϱ_b were utilized, since these parameters showed high correlation with the grain size distributions. Assuming a linear relationship

$$\log_{10}P(d_g)^{[p]} = \boldsymbol{M}\,\vec{p} \tag{7}$$

where $\log_{10}P(d_g)^{[p]}$ is the predicted mass fraction of the soil with a diameter $\leq d_g$, and Matrix $\boldsymbol{M}$ is formed of column vectors of each measured parameter, multiple linear regression technique was used to determine the column vector $\vec{p}$ containing the linear factors. Once vector $\vec{p}$ is determined from Eq. (7) it can be used to directly transform further CPT measurements into estimated values of the CDF, if the assumption of a linear functionality remains valid. For the Krauthausen test site about 250 locations (at B07, B22, and B32) are used to estimate the linear coefficients in Eq. (7). Compared to the bi-variate regressions, the multiple regression approach showed obviously better correlation between CPT measurements and grain size distributions, as it is quantified by the r multiple correlation coefficients $P(d_g)$, $\chi_{(p(d_g)^*,\ p(d_g))}$ (Tables 5, 6 and 7).

As examples, two empirical relationships, set up by multiple regression, are given in the following. First, the estimation of the cumulative grain size distribution for a grain diameter of 0.05 mm ($P(0.05)$), that is the silt to fine sand transition, and, second, the estimation of the diameter of the CDF's 20th percentile (d_{20}):

$$\log_{10}P(0.05)^{[p]} = -3.59\cdot10^{-3}c_r + 5.89\cdot10^{-4}\gamma - 0.31\varrho_b - 1.03 \tag{8}$$

and

$$\log_{10}d_{20} = 1.31\cdot10^{-2}c_r - 5.04\cdot10^{-4}\gamma + 1.14\varrho_b - 5.91. \tag{9}$$

Empirical relations like those in Eqs. (8) and (9) can be found for all the grain diameters of the PDF and CDF and all percentiles. The quality of the relation between the 'true' grain size distribution data from sieving analysis and the estimates from CPT is quantified by the multivariate correlation coefficients χ as well as by the standard deviation of the errors σ. The values for both are shown in Tables 5, 6 and 7. From the respective estimation errors standard deviations of

Table 6
Results of correlation analyses at Krauthausen test site: Bi-variate correlation coefficients between the cumulative grain size distribution (CDF) from sieving and CPT data, including mechanical resistance, c_r, natural gamma activity, γ, bulk density, ϱ_b, matrix density, ϱ_m, and water content, θ

d_g [mm]	0.002	0.01	0.02	0.05	0.1	0.2	0.5	1	2	5	20
c_r	−0.68	−0.61	−0.58	−0.61	−0.60	−0.58	−0.54	−0.46	−0.38	−0.37	−0.34
γ	0.72	0.78	0.80	0.81	0.78	0.69	0.35	0.04	−0.12	−0.13	−0.09
ρ_b	−0.60	−0.56	−0.55	−0.57	−0.52	−0.47	−0.42	−0.35	−0.28	−0.26	−0.25
θ	−0.23	−0.37	−0.42	−0.40	−0.38	−0.28	0.12	0.42	0.49	0.48	0.39
ρ_m	−0.39	−0.26	−0.22	−0.25	−0.22	−0.24	−0.44	−0.56	−0.55	−0.53	−0.48
$\chi_{(P(d_g)^*,\ P(d_g))}$	0.79	0.81	0.81	0.83	0.79	0.72	0.59	0.63	0.65	0.64	0.56
$\sigma_{(P(d_g)^*-P(d_g))}$	0.16	0.16	0.18	0.19	0.20	0.21	0.21	0.18	0.16	0.12	0.04

Parameter $\chi_{(P(d_g)^*,\ P(d_g))}$ denotes the multivariate correlation coefficient between cumulative grain size probability distribution from sieving and it's estimation based on CPT data. Parameter $\sigma_{(P(d_g)^*-P(d_g))}$ denotes the standard deviation of the difference between the multivariate estimate and the 'true' cumulative grain size distribution, i.e. the standard deviation of the error.

Table 7
Results of correlation analyses at Krauthausen test site: Bi-variate correlation coefficients between the percentiles of the cumulative grain size distribution (CDF) from sieving and CPT data, including mechanical resistance, c_r, natural gamma activity, γ, bulk density, ϱ_b, matrix density, ϱ_m, and water content, θ

	d_{10}	d_{20}	d_{30}	d_{40}	d_{50}	d_{60}	d_{70}	d_{80}	d_{90}
$<d_{\%}>$ [mm]	0.14	0.36	0.73	1.2	1.8	2.7	4.1	6.4	11.2
c_r	0.67	0.68	0.63	0.57	0.55	0.52	0.48	0.48	0.48
γ	−0.83	−0.69	−0.41	−0.27	−0.24	−0.18	−0.15	−0.17	−0.21
ρ_b	0.58	0.62	0.55	0.50	0.49	0.47	0.44	0.44	0.45
θ	0.33	0.17	−0.11	−0.20	−0.22	−0.24	−0.25	−0.21	−0.16
ρ_m	0.31	0.44	0.54	0.56	0.56	0.56	0.54	0.53	0.49
$\chi_{(p(d_g)^*,\ p(d_g))}$	0.87	0.79	0.69	0.64	0.63	0.61	0.59	0.57	0.55
$\sigma_{(p(d_g)^*-p(d_g))}$	0.28	0.32	0.38	0.43	0.45	0.47	0.48	0.48	0.45

Parameter $\chi_{(d_{\%}^*,\ d_{\%})}$ denotes the multivariate correlation coefficient between percentiles of the cumulative grain size probability distribution from sieving and it's estimation based on CPT data. Parameter $\sigma_{(d_{\%}^*-d_{\%})}$ denotes the standard deviation of the difference between the multivariate estimate and the 'true' percentiles of the cumulative grain size distribution, i.e. the standard deviation of the error.

the PDF, $0.16<\sigma<0.53$ (Table 5), and CDF, $0.04>\sigma<0.21$ (Table 6), it can be recognized, that the CDF estimation is more accurate for all grain sizes. Therefore the relationship between CPT measurements and the CDF were used for the grain size distribution estimation. The result is presented in Fig. 8g, and as expected it shows a good coincidence with the 'true' grain size distribution in Fig. 8f for the clay and silt fraction. However, the proportion sand to gravel fraction is not well estimated. In particular, the estimated gravel fraction is underestimated, while the sand fraction is overestimated.

5.2. Validation of the estimated grain size distributions

Vereecken et al. (2000) analyzed the grain size distribution of 250 soil samples obtained from undisturbed cores from the boreholes B07, B22 and B32 from test site Krauthausen. These grain size distributions were used for the multiple regression analysis of Section 5.1. However, 142 more sediment samples, which were taken from 31 boreholes at the elevation interval 90 m–92 m above MSL were analyzed by (Vereecken et al., 2000). All these grain size distributions will be used in the following to validate the reliability of the estimated grain size distributions based on the CPT data. Although it was shown in Section 4.2 that the material parameters disclose an anisotropic correlation structure in horizontal direction, we assume isotropy in horizontal direction in this and the following Section, due to the limited number of sample locations in Vereecken et al. (2000).

For the integrated analysis, two distinct data sets each containing 'true' sieving data and estimated grain size distributions, based on CPT data, both from the elevation interval of 90 m to 92 m above MSL were prepared. The first data set contains the local distribution of the CDF of the Vereecken et al. (2000) data at a grain diameter of 0.05 mm, that is the clay and silt fractions mass, and their estimate according to Eq. (8). For the second data set the 20th percentile is determined from the CDF of the Vereecken et al. (2000) data as well as estimated using Eq. (9).

For the analysis of the horizontal spatial isotropic correlation structure, variograms for all data sets were calculated using a lag increment of 1 m and a lag tolerance of ±0.75 m, while a lag increment of 0.1 m and a lag tolerance of ±0.1 m were used for vertical variogram calculation.

Fig. 9 shows the results for the first data set. Comparing the probability distributions of $P(0.05)$ and its estimation, shown in Fig. 9a and c, respectively, their dissimilarity is obvious. The estimator of $P(0.05)$ results in a log-normal shaped mass fraction distribution, predicting a clay and silt content of 2 to 5%. Sieve analysis discloses a broader distribution of $P(0.05)$. The experimental variograms of the horizontal direction are shown in Fig. 9b. The variogram of the sieving data shows the semivariances fluctuating around the sill level, without a slope of the semivariances for smaller lag distances. Although the sill and the fluctuations around the sill are smaller, also the semivariances of the CPT data disclose values of the sill level, without a slope for smaller lag distances. Both variogram data may be interpreted as part of the exponential curve close to the sill. In this case the only information obtained from the variogram analysis is that the range a in both supposed variograms is smaller than 3 m. However, one has to keep in mind, that both results have limited validity, since the assumption of an isotropic layer is violated as mentioned before.

The vertical variograms are shown in Fig. 9d, which are, in contrast to the horizontal variograms, explicable

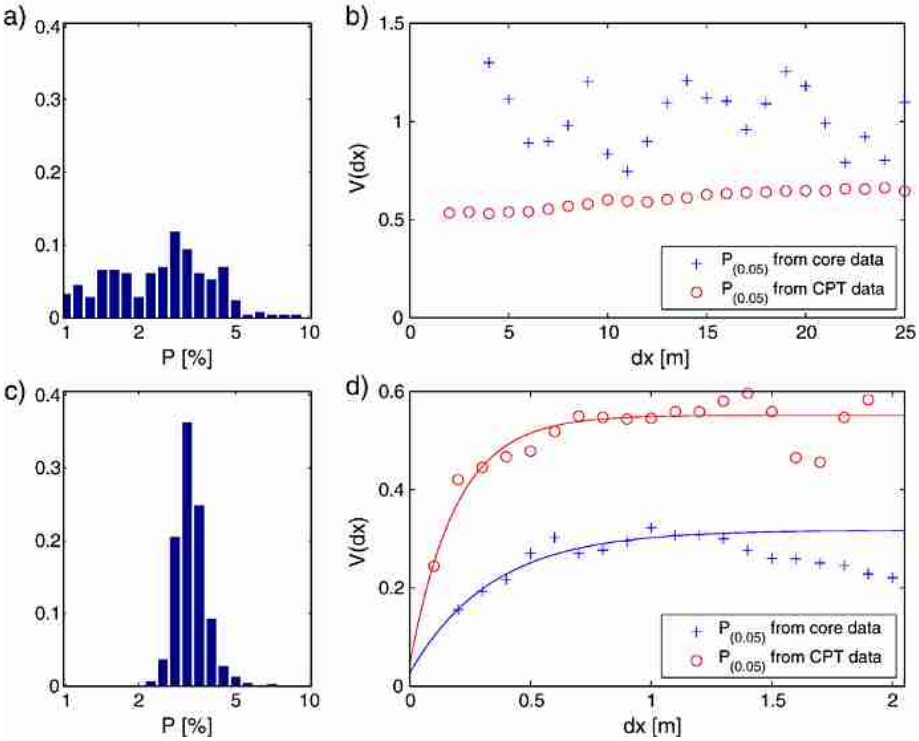

Fig. 9. Comparison of CPT data and core sample data at Krauthausen test site: a) histogram of the mass fraction at grain diameter 0.05 mm, $P(0.05)$, from core sample data, b) horizontal variograms of $P(0.05)$ from CPT and core sample data, c) histogram of $P(0.05)$ values estimated from CPT data, d) vertical variograms of $P(0.05)$ from CPT and core sample data.

by the exponential model. The corresponding fits result in a sill of 0.29 and 0.51, a nugget of 0.03 and 0.04, a correlation length of 0.34 m and 0.19 m, and a spatial range of 1 m and 0.56 m for the value from sieving analysis and CPT estimation, respectively. The differences for nugget, the spatial range and the correlation length are reasonable, with a divergence of factor <1.8. The most striking discrepancy appears in the sill value being smaller for the sieving analysis data. Comparison between variograms in horizontal and vertical direction show the sill value of the CPT estimated data on the same level. This is different for the sieving analysis data, here the sill value of the variogram in horizontal direction is explicitly higher than the one in vertical direction. This indicates a zonal anisotropy for the sieving analysis data, which is missing in the CPT estimated data. We suggest that this is mainly due to the smaller variability in the CPT estimated data, compared to the variability of the sieving analysis data.

The results of the analysis of the second data set is presented in Fig. 10. In contrast to the first data set, the probability distribution of the d_{20} value, shown in Fig. 10a, coincides with the probability of its estimation, shown in Fig. 10c. Both distributions have nearly identical mean and standard deviation, that is $d_{20}=0.65\pm0.24$ mm from sieve analysis and 0.67 ± 0.19 mm estimated from CPT. The variograms in the horizontal direction are shown in Fig. 10b. They are shaped similar to the horizontal variograms discussed above, but now with fluctuating semivariance around a value 0.6 for both d_{20} from sieve analysis and d_{20} estimated from CPT. However, they are again not interpretable with the exponential correlation model aside the fact that the range is $a\leq3$ m. This is probably caused by the isotropic assumption for the anisotropic horizontal correlation structure within this layer.

In contrast, the first data set, the vertical experimental variograms of the d_{20} percentile and its estimation are related, as shown in Fig. 10d. They are both fitted with an exponential variogram model with nugget. The fits result in a sill of 0.39 and 0.49, a correlation length of 0.16 m and 0.36 m, and a spatial range of 0.47 m and 1.07 m for the percentile and its estimation, respectively. A zero nugget was found for both.

Other than the quantitative validation of the quality of the estimation of grain size distribution by correlation coefficients (see Section 5.1), the evaluation of the two data sets shows the application of the methodology

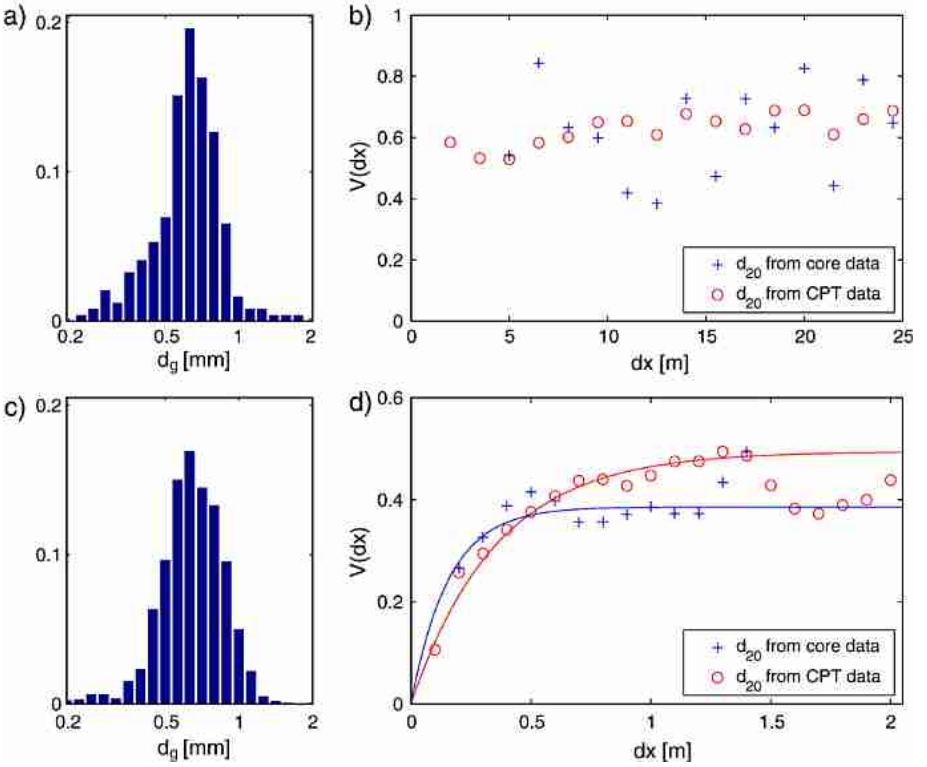

Fig. 10. Comparison of CPT data and core sample data at Krauthausen test site: a) histogram of the 20th percentile, d_{20}, from core sample data, b) horizontal variograms of d_{20} from CPT and core sample data, c) histogram of d_{20} values estimated from CPT data, d) vertical variograms of d_{20} from CPT and core sample data.

proposed together with two data sets from sieving analysis. Comparing the statistics of estimated grain size parameters from CPT measurements with those of sieving analyses in the depth between 90 m and 92 m above MSL, can be stressed as a study of the reliability of the method, independent from the set of quasi-co-located data used in the multivariate regression. Discrepancies between the sieving data based statistics and the CPT data based statistics may be due to several reasons, like different number of measurements, different horizontal resolution or statistical instationarity of the aquifer at Krauthausen test site. However similarities between the data sets sustain the reliability of the statistics of both data sets.

5.3. Estimation of hydraulic conductivity

Since an accurate estimation of the percentile d_{20} can be expected from the CPT survey (see Sections 5.1 and 5.2), it is used in combination with the Bialas formula (see Section 2.2 and Bialas and Kleczkowski (1970)) to obtain the hydraulic conductivity within layers B to E.

Table 8
Estimated hydraulic conductivity within the aquifer layers of Krauthausen test site, including, $<K>$, the mean hydraulic conductivity, $<\log_{10} K>$, the mean of the logarithmic hydraulic conductivity, and σ its standard deviation

	B	C	D	E	D[V]	E[V]
$<K>$ [m/s]	$9.6\cdot10^{-5}$	$9.4\cdot10^{-4}$	$2.5\cdot10^{-4}$	$1.1\cdot10^{-3}$	$7.3\cdot10^{-4}$	$1.4\cdot10^{-3}$
$<\log_{10} K>$	−4.02	−3.03	−3.60	−2.98	−3.10	−2.85
σ	0.97	0.69	0.45	0.42	1.48	1.76
λ_h [m]	9.45	0.30	5.00	1.75	–	6.6(±4.7)
λ_v [m]	–	0.40	0.60	0.36	–	0.6(±0.3)

Parameters λ_h and λ_v are the horizontal and vertical correlation lengths fitted with an exponential model, respectively. The results in columns D[V] and E[V] are taken from Vereecken et al. (2000).

The aquifer consisting of layer C to E has a hydraulic conductivity of $1 \cdot 10^{-3}$ m/s in layers C and E, and of $2.5 \cdot 10^{-4}$ m/s in layer D. The saturated hydraulic conductivity in the unsaturated layer B is predicted to be $1 \cdot 10^{-4}$ m/s. The mean hydraulic conductivities, the mean of the logarithmic hydraulic conductivity, its standard deviation and the correlation lengths are compiled in Table 8. For comparison, the corresponding values of layer D and E from Vereecken et al. (2000), $D^{[V]}$ and $E^{[V]}$, are also shown in Table 8. In Vereecken et al. (2000) the hydraulic conductivity statistics are estimated based on local hydraulic conductivities derived from 279 sediment samples using grain size analysis and the formula of Seiler (1973)(see Section 2.2). As can be seen from Table 8, the mean values of the hydraulic conductivities within the layers are in good agreement, while the variabilities of the CPT estimation are lower than the variabilities observed by Vereecken et al. (2000). The underestimation of the variability connected with the hydraulic conductivity estimation based on the CPT measurements is presumably a consequence of the utilized linear relationships. Those are based on a multiple regression analysis with correlation coefficient of 0.79.

Vereecken et al. (2000) reports an isotropic estimation of the horizontal and vertical correlation lengths within layer E. For comparison purposes, isotropic variograms were also computed for the CPT estimated hydraulic conductivities. Fitting by the exponential model (Eq. (5)), like in Vereecken et al. (2000) results in smaller correlation length estimations from CPT data, compared to those of Vereecken et al. (2000). However, both investigations result in the same order of magnitude, regarding horizontal and vertical correlation length.

6. Summary and conclusions

A spatially highly resolved CPT survey was performed at the test site Krauthausen, Germany, to investigate the spatial variability of physical soil properties in the aquifer, including the mechanical resistance, c_r, natural gamma activity, γ, bulk density, ϱ_b, matrix density, ϱ_m, water content, θ, and electrical resistivity, ρ. Based on the analysis of the CPT measurements, following results can be summarized:

The Krauthausen test site's heterogeneity is dominated by a planar stratification. Regarding this aspect, the CPT results conformed in general with the geological profile from drillings. A layer-wise characterization of the parameter's spatial variability disclosed a structure including statistical anisotropy between horizontal and vertical direction and an azimuthal anisotropy of the spatial range in the horizontal direction. The horizontal direction of the maximum range was similar for all measured material parameters and all investigated layers of the aquifer, and corresponded to the main flow direction of the fluvial sedimentary system. Based on an exponential correlation function, spatial ranges of typical 5–9 m, were found in the horizontal, and ranges of about 1 m in the vertical direction.

Although not measured during the CPT survey, a multiple regression analysis provided the estimation of local grain size distributions based on CPT measurements. The measured CPT data and characteristic points of measured grain size distributions showed correlation coefficients ≥ 0.7, at least for small grain sizes up to fine sands. The correlation coefficients found for coarser grain sizes indicated a connection of lower accuracy, but useful for classification. Subsequent comparison between uni-variate and spatial statistics of estimated and measured 20th percentile of local grain size distributions showed reasonable agreement.

Supposing the link between grain size distribution and hydraulic conductivity to be valid, as found in various references, the hydraulic conductivity at each CPT measurement location was estimated using the formula of Bialas and Kleczkowski (1970). This formula is based on the 20th percentile, whose estimation by CPT was found to be of high accuracy in terms of a high correlation coefficient. Hydraulic conductivity statistics based on CPT were in good agreement with a prior investigation based on sediment samples, in terms of the mean. Variance and correlation–length were underestimated by the CPT based estimation, but were of the same order of magnitude as statistics based on sediment samples. Moreover, the CPT based estimation of the mean hydraulic conductivity agreed with the hydraulic conductivity based on a pumping test performed in a former study.

Following conclusions can be drawn from the obtained results: The CPT method was found to be a promising tool for a spatially dense sampled investigation of the subsoil's heterogeneity in various physical parameters, including the mechanical resistance, c_r, natural gamma activity, γ, bulk density, ϱ_b, matrix density, ϱ_m, water content, θ, and electrical resistivity, ρ. Using multiple regression, a reliable link between CPT measurements and the sediment grain size distributions could be established. Using the empirical formula of Bialas and Kleczkowski (1970) the grain size distribution could be related to the hydraulic conductivity. Finally an integrated analysis of CPT based estimated hydraulic conductivities and hydraulic

conductivities of former investigations, proposed this methodology to be viable.

Acknowledgements

This scientific article is dedicated to the memory of our colleague and friend Imre Fejes (1943-2006). Henceforce he resides in heaven and lives in our hearts. We wish to thank the team of Janos Stickel from ELGOSCAR 2000, Budapest, Hungary, who performed the Cone Penetration Tests. This work is funded partly by the NATO Collaborative Linkage Grant No. CLG-EST-979868.

References

Alyamani, M.S., Sen, Z., 1993. Determination of hydraulic conductivity from complete grain-size distribution curves. Ground Water 31 (4), 551–555.

Beyer, W., 1964. Zur Bestimmung der Wasserdurchlässigkeit von Kiesen und Sanden aus der Kornverteilungskurve. Wasserwirtsch. Wassertech. 14, 165–168.

Bialas, Z., Kleczkowski, A.S., 1970. Über den praktischen Gebrauch von einigen empirischen Formeln zur Berechnung des Durchlässigkeitskoeffzienten K. Archivum Hydrotechniki, Warschau.

Bowders, J., Daniel, D.E., 1994. Cone penetration technology for subsurface characterization. Geotech. News 12 (3), 24–29.

Campanella, R.G., Weemees, I., 1990. Development and use of an electrical resistivity cone for groundwater contamination studies. Can. Geotech. J. 27 (5), 557–567.

Chilès, J.P., Delfiner, P., 1999. Geostatistics — Modeling Spatial Uncertainty. John Wiley and Sons, New York.

Deutsch, C.V., 2002. Geostatistical Reservoir Modeling. Oxford University Press, Oxford.

Döring U., 1997. Transport der reaktiven Stoffe Eosin, Uranin und Lithium in einem heterogenen Grundwasserleiter, PhD thesis, Christian-Albrechts Universität Kiel, Kiel, Germany.

Eggelston, J., Roistacer, S., 2001. The value of grain-size hydraulic conductivity estimates: comparison with high resolution in-situ field hydraulic conductivity. Geophys. Res. Lett. 28 (22), 4255–4258.

Englert A., 2003. Measurement, Estimation and Modelling of Groundwater Flow Velocity at Krauthausen Test Site, PhD thesis, RWTH Aachen, Aachen, Germany.

Fejes, I., Jósa, E., 1990. The engineering geophysical sounding method: principles, instrumentation, and computerised interpretation. Geotechnical and Environmental Geophysics, Volume II: Environmental and Groundwater. SEG, Tulsa, Oklahoma, pp. 321–331.

Fejes, I., Szabadváry, L., Veró, L., Stickel, J., 1997. Geophysikalische Penetrationssondierungen, Methodenhandbuch Deponienuntergrund. Band Geophysik. Springer, Berlin, pp. 897–922.

Goovaerts, P., Jacquez, G.M., 2004. Accounting for regional background and population size in the detection of spatial clusters and outliers using geostatistical filtering and spatial neutral models: the case of lung cancer in Long Island, New York. Int. J. Health Geogr. 3 (14). doi:10.1186/1476-072X-3-14.

Gringarten, E., Deutsch, C.V., 2001. Teacher's aide: variogram interpretation and modeling. Math. Geol. 33 (4), 507–534.

Hazen, A., 1892. Physical Properties of Sands and Gravels with Reference to Use in Filtration. Report to Mass. State Board of Health, p. 539.

Hubbard, S., Chen, J., Peterson, J., Majer, E.L., Williams, K.H., Swift, D.J., Mailloux, B., Rubin, Y., 2001. Hydrogeological characterization of the South Oyster Bacterial Transport Site using geophysical data. Water Resour. Res. 37 (10), 2431–2456.

Isaaks, E., Srivastava, R.M., 1989. An Introduction into Applied Geostatistics. Oxford university press, Oxford.

Kozeny, J., 1953. Hydraulik. Springer–Verlag, Wien.

Lunne, T., Robertson, P.K., Powell, J.J.M., 1997. Cone Penetration Testing in Geotechnical Practice. Blackie Acad. and Prof., New York.

Russo, D., Zaidela, J., Laufera, A., 2004. Numerical analysis of transport of interacting solutes in a three-dimensional unsaturated heterogeneous soil. Vadose Zone J. 3, 1286–1299.

Seiler, K.P., 1973. Durchlässigkeit, Porosität und Kornverteilung quartärer Kies-Sand-Ablagerungen des bayerischen Alpenvorlandes. GWF Tech. Rep. 114 (8), 353–358.

Slichter, C.S., 1899. Theoretical investigations of the motion of ground waters. U.S. Geological Survey 19th Annual Report, Part 2.

Sperry, J.M., Peirce, J.J., 1995. A model for estimating the hydraulic conductivity of granular material based on grain shape, grain size, and porosity. Ground Water 33 (6), 892–898.

Stein, M.L., 1999. Interpolation of Spatial Data: Some Theory for Kriging. Springer Verlag, Berlin.

Telford, W.M., Geldart, L.P., Sheriff, R.E., 1990. Applied Geophysics, 2nd edition. Cambridge University Press, New York.

Tillmann, A., 2005. Cone Penetration Tests (CPT) on the Krauthausen Test Site. Part I: Data Acquisition and Preliminary Interpretation of the Surveys 2003 and 2004, Bericht des Forschungzentrums Jülich GmbH, Jülich. http://nbn-resolving.de/urn/resolver.pl?urn=urn:nbn:de:0001-00288 online available.

Tillmann, A., Nyari, Z., Fejes, I., Vanderborght, J., Vereecken, H., 2004. Cone penetration tests for investigation of heterogeneity in an aquifer at Krauthausen. EAGE 66th Conference and Exhibition, Extended Abstracts European Association of Geoscientists and Engineers, Paris, p. P-157.

Vanderborght, J., Vereecken, H., 2002. Estimation of local scale dispersion from local breakthrough curves during a tracer test in a heterogeneous aquifer: the Lagrangian approach. J. Contam. Hydrol. 54, 141–171.

Vereecken, H., Döring, U., Hardelauf, H., Jaekel, U., Neuendorf, O., Schwarze, H., Seidemann, R., 1999. Analysis of Solute Transport in a Heterogeneous Aquifer: The Krauthausen Field Experiment. 1. Experimental Set-up, Sediment Characterization and, Moment Analyses, Internal Report No. 500798. Forschungszentrum Jülich, Jülich, Germany.

Vereecken, H., Döring, U., Hardelauf, H., Jaekel, U., Hashagen, U., Neuendorf, O., Schwarze, H., Seidemann, R., 2000. Analysis of solute transport in a heterogeneous aquifer: the Krauthausen field experiment. J. Contam. Hydrol. 45, 329–358.

Vuković, M., Soro, A., Miladinov, D., 1992. Determination of hydraulic conductivity of porous media from grain-size composition. Water Resources Publications, Littleton, CO, pp. 329–358.